Three-Dimensional Simulation of Femur Bone and Implant in Femoral Canal using Finite Element Method

Somkid Amornsamankul, Kamonchat Kaorapapong, Benchawan Wiwatanapataphee

Abstract— In this paper, a mathematical model is developed to simulate three-dimensional femur bone and femur bone with implant in the femoral canal, taking into account stress distribution and total displacement during horizontal walking. The equilibrium equations are used in the model. Realistic domain are created by using CT scan data. Different cases of static loads and different boundary conditions are used in the simulation. The finite element method is utilized to determine total displacement and Von Mises Stress. The influences of human weight during horizontal walking are investigated. This model will give the useful for surgeon in femur surgeries. The results show that higher weight provides higher total displacement. And it is found that the Von Mises stress affects the lateral femur.

Keywords— Femur bone, Finite element method, Three dimensional simulation, Mathematical modeling, Implant in the femoral canal.

Fig. 1. Three-dimensional geometry of fumer bone and its finite element mesh.

I. Introduction

IN several centuries, human has tried to understand all parts of human body. Biologist and medical staff did a lot of experiments for this topics. The cost, operation time and lead time were used to carry out the knowledge. Since the computer era come to the world. Mathematicians have applied mathematical models to explain human organism such as brain, heart, blood, lung and bone. These studied are very useful for orthopedic surgeon.

Femur is a leg bone which is the most important organism in human body. In vitro experiments were conducts to analyse the distribution of stress across the neck of the femur; however, the shear stress distribution was not satisfy [1], [2]. Finite element models were developed foe normal and osteoarthritic

S. Amornsamankul is with Department of Mathematics, Faculty of Science, Mahidol University, Rama VI road, Bangkok 10400, Thailand and is with the Centre of Excellence in Mathematics, the Commission on Higher Education, 328 Si Ayutthaya Road, Bangkok 10400, Thailand. (corresponding author, phone: 662-201-5339; fax: 662-201-5343; email: scsam@mahidol.ac.th)

K. Kaorapapong is with Department of Mathematics, Faculty of Science, Mahidol University, Rama VI road, Bangkok 10400, Thailand and is with the Centre of Excellence in Mathematics, the Commission on Higher Education, 328 Si Ayutthaya Road, Bangkok 10400, Thailand. (email: g5237091@student.mahidol.ac.th)

B. Wiwatanapataphee is with Department of Mathematics, Faculty of Science, Mahidol University, Rama VI road, Bangkok 10400, Thailand and is with the Centre of Excellence in Mathematics, the Commission on Higher Education, 328 Si Ayutthaya Road, Bangkok 10400, Thailand. (phone: 662-201-5540; fax: 662-201-5343; email: scbww@mahidol.ac.th)
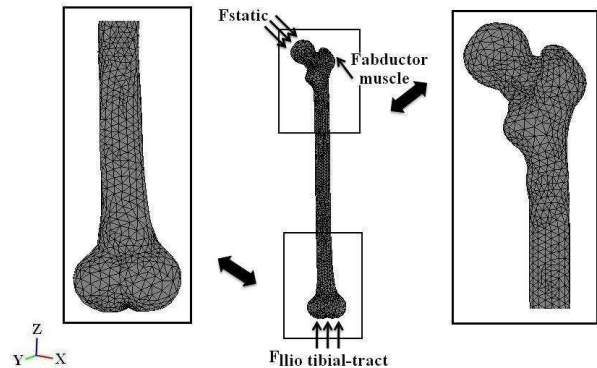
femur [3]. Some researches developed three dimensional mathematical models to investigate the geometry of femur and stress [4], [5]. Krauze [6] also studied a numerical simulation for stresses and displacement in femur in a living and a dead phase. The influence of mechanical properties of bone tissues were also investigated in their studies. The femur fractures in case of frontal car accidents are determined [7]. It is also found that the boundary conditions and load conditions are affected to the numerical simulations significantly [8]. Moreover, modular adaptive implants for fractured bone and X-ray based technique for bone fracture problem are developed [9], [10]. It is founded that CT scan realistic bone models are important for the simulation. That means the realistic geometry of femur bone with implant is still a subject for active research.

This paper aims to construct a completed three-dimensional femur bone and implant in femoral canal based on CT scan data. The mimics commercial software and FEMLEB commercial software are used. The finite element method is applied to carried out stress distribution and total displacement. The rest of the paper is organized as follow. Section 2 describes the governing equations of the mathematical models. Two domains, boundary conditions and five different cases of static load are shown in section 3. The results and discussion are also shown in Section 4. Finally, Section 5 presents conclusions and future works.
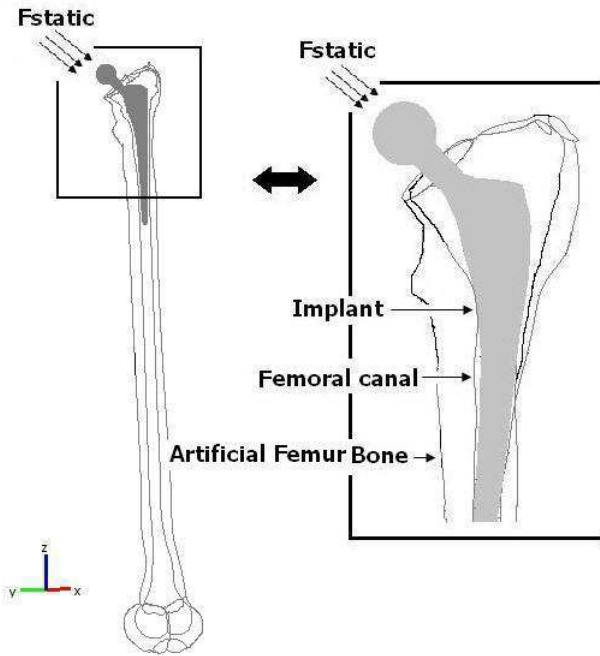
Fig. 2. The artificial femur bone geometry consists femural canal bone and implant. Forces on the head implant.
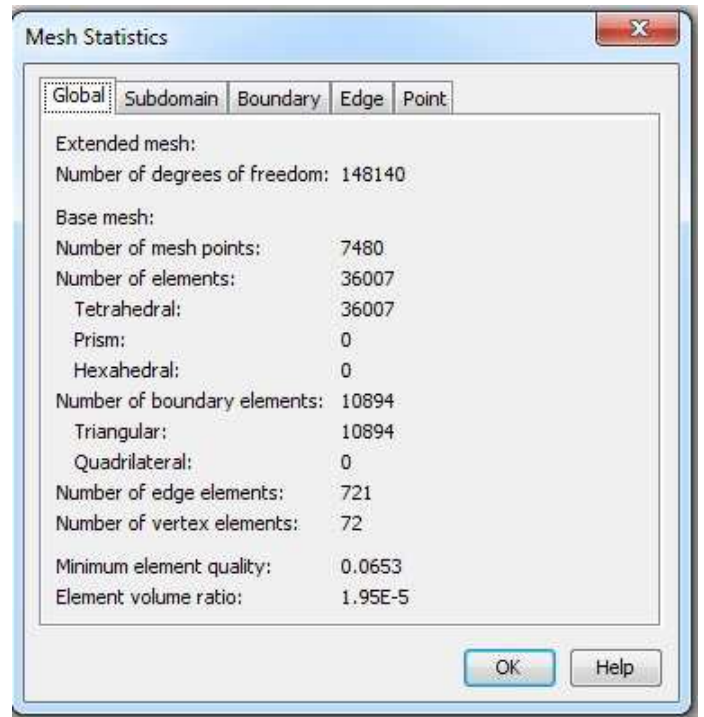
Fig. 4. Mesh statistic of the artificial femur bone geometry.

TABLE I

THE EXPERIMENT PARAMETERS USED IN THE NUMERICAL SIMULATION OF ARTIFICIAL FEMUR BONE [11].

Parameters	Femur	Units
Density (ρ)	2000	kg/m^3
Young's modulus (E)	2.130	GPA
Poisson's ratio (ν)	0.3	$-$
Yield strength	1.48×10^8	Pa
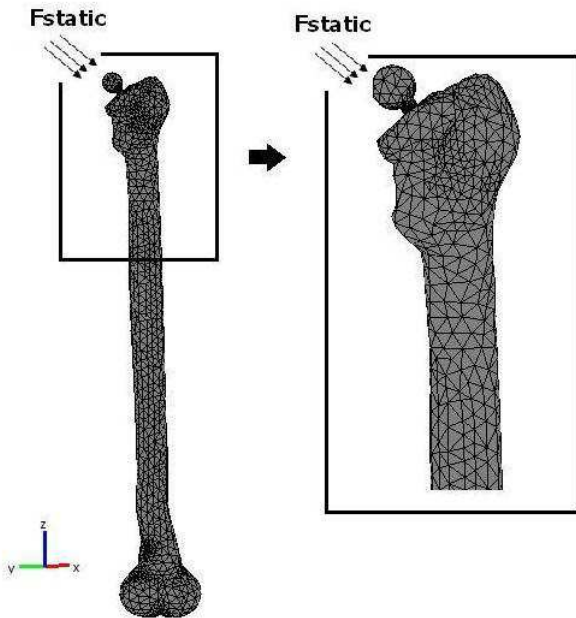
Fig. 3. Mesh of the artificial femur bone geometry consists of 36,007 tetrahedral elements and 148,140 degrees of freedom. Forces on the head implant.

II. MATHEMATICAL MODEL

Three-dimensional model of the right femur was constructed using CT scan data of a human femur. Fig. 1 shows the complete geometry of the right femur bone of length 50 cm with forces acting on the head and the end of femur. Mesh of the femur bone geometry consists of 17,495 tetrahedral elements and 87,288 degrees of freedom. Implant and femoral canal in artificial femur bone was constructed as shown in Fig. 2 base on real domain. Fig. 3 shows the complete geometry of the femur bone with forces acting on the head of bone implant. Mesh of the artificial femur bone geometry consists of 36,007 tetrahedral elements and 148,140 degrees of freedom as shown in Fig. 4.

The bone is assumed to be a Von Mises elasto-plastic material. From the principles of continuum mechanics, the field equations governing the displacement and stress fields

TABLE II

THE EXPERIMENT PARAMETERS USED IN THE NUMERICAL SIMULATION
OF FEMORAL CANAL [11].

Parameters	Femoral canal	Units
Density (ρ)	1100[65]	kg/m^3
Young's modulus (E)	2.28	GPA
Poisson's ratio (ν)	0.3	–
Yield strength	4.38×10^4	Pa

TABLE III

THE EXPERIMENT PARAMETERS USED IN THE NUMERICAL SIMULATION
OF IMPLANT [11].

Parameters	Implant	Units
Density (ρ)	4420[25]	kg/m^3
Young's modulus (E)	210	GPA
Poisson's ratio (ν)	0.3	–
Yield strength	7.20×10^5	Pa

in the femur bone include the stress equilibrium equations as follows:

$$\sigma_{ij,j} + f_i = 0 \quad (i = 1, 2, 3) \tag{1}$$

$$\varepsilon_{ij}(\vec{u}) = \frac{1}{2}(u_{i,j} + u_{j,i}), \tag{2}$$

$$\sigma_{i,j} = (C_{ep})_{ijrs}\varepsilon_{rs}, \tag{3}$$

where σ and ε denote respectively the stress tensor and the strain tensor, $\vec{u}$ is displacement, f_i is body force and $(C_{ep})_{ijrs}$ is a tensor of elastic constants, or a modulus which are independent of stress or strain.

The parameters which is shown by Table 1,2 and 3 used in the numerical simulation. For the domain as shown in Fig. 1, we impose three boundary conditions based on the human's weight as follows [12]:

(I). $F_{dynamic}$: $F_x = 234\,N,\ F_y = 385\,N,$ $F_z = -1652\,N$

$F_{abdductor}$: $F_x = 0\ N,\ F_y = 0.8\,N,$ $F_z = -1.937\,N$

$F_{lliotibial-tract}$: $F_x = 0\ N,\ F_y = 0\,N,$ $F_z = 350\,N$

(II). $F_{dynamic}$: $F_x = 334.8\,N,\ F_y = 550\,N,$ $F_z = -2360\,N$

$F_{abdductor}$: $F_x = 0\ N,\ F_y = 1.142\,N,$ $F_z = -2.8\,N$

$F_{lliotibial-tract}$: $F_x = 0\ N,\ F_y = 0\,N,$ $F_z = 500\,N$

(III). $F_{dynamic}$: $F_x = 669.6\,N,\ F_y = 1100\,N,$ $F_z = -4720\,N$

$F_{abdductor}$: $F_x = 0\ N,\ F_y = 2.285\,N,$ $F_z = -5.6\,N$

$F_{lliotibial-tract}$: $F_x = 0\ N,\ F_y = 0\,N,$ $F_z = 1000\,N$

The loads (I), (II) and (III) represent terminal stance during horizontal walking in which each person has the weight of 70, 100 and 200 kg, respectively.

In order to simulate the stress field corresponding to the patient activities for the fumer with implant as shown in fig. 2 , we impose two types of boundary conditions. On the distal epiphysis (the base) displacement is restrained. On the implant head external point load is imposed to simulate the force acting on the object corresponding to patient's activity. In this domain, we impose two different cases of static loads as shown in table IV

TABLE IV

THE EXPERIMENT PARAMETERS USED IN THE NUMERICAL SIMULATION
OF IMPLANT

Force	Implant Load (I)	Implant Load (II)	Unit
F_x	0	1.4×10^3	N/m^3
F_y	0	1×10^3	N/m^3
F_z	-3×10^3	-4.8×10^3	N/m^3

The implant load (I) approximate the peak gait load for a 70 kg person during normal walk [13] and the implant load (II) approximate the terminal stance during horizontal walking [14].

III. FINITE ELEMENT FORMULATION

To solve the boundary value problem numerically by the finite element method, we multiply equation (1) by a weighting function $v(x)$. Setting the total weighted residual error to zero, that is,

$$\int_\Omega \sigma_{ij,j} v_i d\Omega = -\int_\Omega f_i v_i d\Omega \qquad (4)$$

From the symmetry of $\sigma_{ij,j}$, we have

$$\sigma_{ij,j} v_i = (\sigma_{ij} v_i)_{,j} - \sigma_{ij} v_{i,j} \qquad (5)$$

Substituting equation (5) into (4) and using the divergence theorem, we obtain

$$\int_\Omega \sigma_{ij} v_{i,j} d\Omega = \int_\Omega f_i v_i d\Omega + \int_{\partial\Omega} \sigma_{ij} n_j v_i ds \qquad (6)$$

Using the boundary condition, we get

$$\int_\Omega \sigma_{ij} v_{i,j} d\Omega = \int_\Omega f_i v_i d\Omega + \int_{\partial\Omega} F\delta(r - r_0) v_i ds \qquad (7)$$

Let

$$u = \begin{bmatrix} u_x \\ u_y \\ u_z \end{bmatrix}, v = \begin{bmatrix} v_x \\ v_y \\ v_z \end{bmatrix},$$

$$\varepsilon = \begin{bmatrix} \varepsilon_x \\ \varepsilon_y \\ \varepsilon_z \\ 2\varepsilon_{xy} \\ 2\varepsilon_{yz} \\ 2\varepsilon_{zx} \end{bmatrix},$$

$$\sigma = \begin{bmatrix} \sigma_{xx} \\ \sigma_{yy} \\ \sigma_{zz} \\ \sigma_{xy} \\ \sigma_{yz} \\ \sigma_{zx} \end{bmatrix},$$

$$f = \begin{bmatrix} f_1 \\ f_2 \\ f_3 \end{bmatrix},$$

$$D = \begin{bmatrix} \frac{\partial}{\partial x} & 0 & 0 \\ 0 & \frac{\partial}{\partial y} & 0 \\ 0 & 0 & \frac{\partial}{\partial z} \\ \frac{\partial}{\partial y} & \frac{\partial}{\partial x} & 0 \\ 0 & \frac{\partial}{\partial z} & \frac{\partial}{\partial x} \\ \frac{\partial}{\partial z} & 0 & \frac{\partial}{\partial x} \end{bmatrix}.$$

we then have

$$\sigma_{ij} v_{i,j} = \frac{1}{2}\sigma_{ij}(v_{i,j} + v_{j,i}) = \sigma_{ij}\varepsilon_{ij}(v) \qquad (8)$$

and hence (8) becomes

$$\int_\Omega Dv^T CDu d\Omega = \int_\Omega v^T f d\Omega + \int_{\partial\Omega_2} v^T g ds. \qquad (9)$$

Therefore, the variational statement for the BVP can be stated as follows:

Find $u \in V$ such that

$$a(u,v) = L(v) \quad \forall v \in V \qquad (10)$$

where

$$a(u,v) = \int_\Omega (Dv)^T C(Du) d\Omega$$

$$L(v) = \int_\Omega v^T f d\Omega + v^T(r_o)F$$

$$V = \{v \in [H_1(\Omega)]^3 \mid v = 0 \ on \ \partial\Omega_1\}.$$

To find the numerical solution of the variational boundary value problem, we pose the problem in an N-dimensional subspace with basis function $\{\phi_i\}_{i=1}^N$, and approximate u and v by

$$u = \sum_{j=1}^n \Phi_j u_j, \quad v = \sum_{j=1}^n \Phi_j v_j, \qquad (11)$$

where

$$\Phi_j = \begin{bmatrix} \phi_j & 0 & 0 \\ 0 & \phi_j & 0 \\ 0 & 0 & \phi_j \end{bmatrix}, u_j = \begin{bmatrix} u_{xj} \\ u_{yj} \\ u_{zj} \end{bmatrix}.$$

Substituting into and noting that v_i is arbitrary, we have

$$a(\Phi_j, \Phi_i)u_j = L(\Phi_i) \qquad (i,j = 1,2,\ldots,N), \qquad (12)$$

which represents a system of 3N equations in terms of 3N unknowns

$$\{(u_{xj}, u_{uj}, u_{zj})\}_{j=1}^N.$$

The system is a nonlinear system and can be solved by the quasi-Newton method.

IV. RESULTS AND DISCUSSION

In the first domain as shown in Fig. 1, the effect of the human's weight on the total displacement and von Mises stress during horizontal walking have been investigated. In Fig. 5– 7, the total displacement of the loading approximates the peak gait load for a 70 kg, 100 kg and 200 kg person during horizontal walking, respectively. The results show that
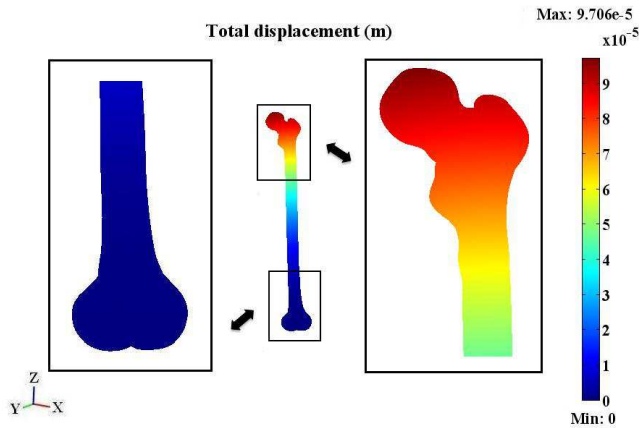
Fig. 5.   Total displacement of the loading approximates the peak gait load for a 70 kg person during horizontal walking.
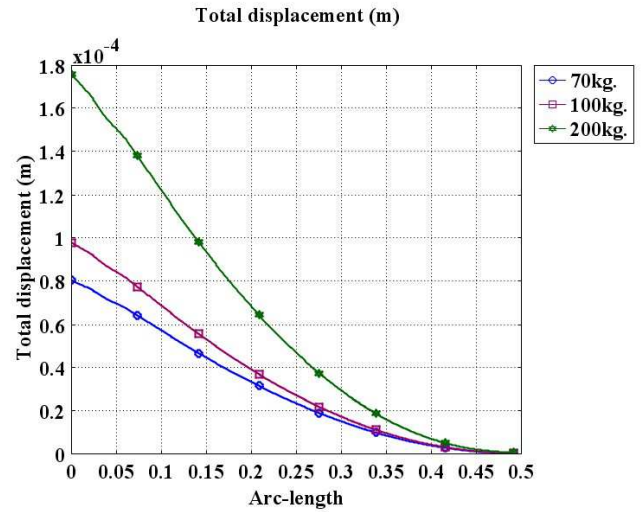
Fig. 8.   Profile of total displacement along the axial of femur bone where the solid-circled line corresponds to the load of 70 kg, the solid-squared line corresponds to the load of 100 kg, and the solid-starred line corresponds to the load of 200 kg.
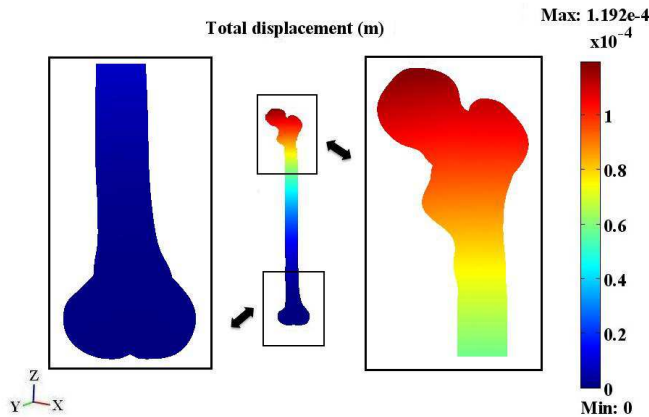
Fig. 6.   Total displacement of the loading approximates the peak gait load for a 100 kg person during horizontal walking.
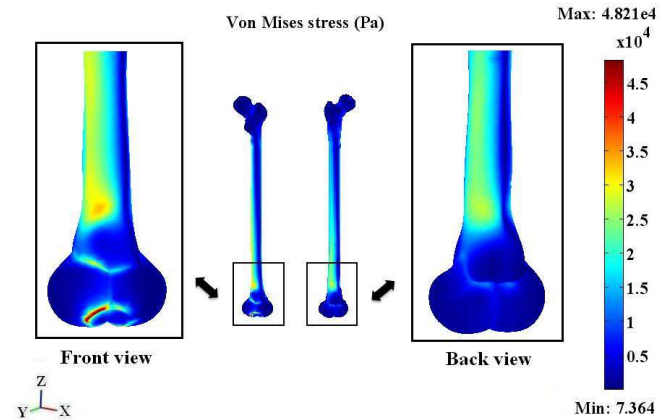
Fig. 9.   Von Mises stress of the loading approximates the peak gait load for a 70 kg person during horizontal walking.
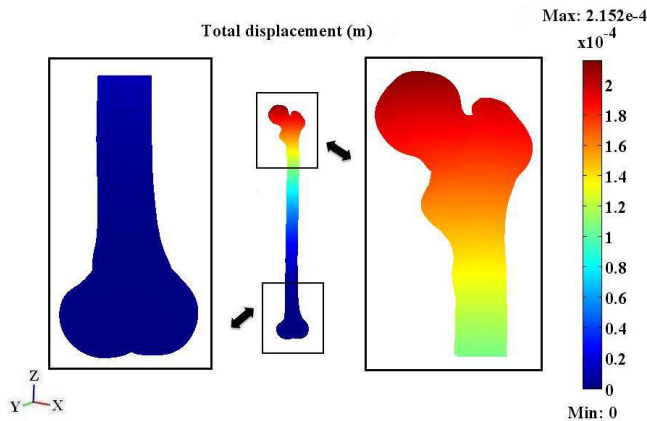
Fig. 7.   Total displacement of the loading approximates the peak gait load for a 200 kg person during horizontal walking.

high displacement appears at the head of the femur bone and the lower displacement occurs at the end of the femur bone. The total displacement for different human weights are compared in Fig. 8. It is found that higher weight provides higher total displacement and lower weight provides lower total displacement.

Front view and back view of Von Mises stress are shown in Fig. 9– 11. The results indicate that higher Von Mises Stress is located at the front view of the end of femur. Additionally, the Von Mises stress indirectly affects the lateral femur bone.

The computational domain as shown in Fig. 3 is separable in space into 36,007 tetrahedral elements and 148,140 degrees of freedom. The material properties for the implant are : density $\rho = 4420\ kg/m^3$, Young's modulus $E = 210\ GPA$, Poisson's ratio $\nu = 0.3$ and yield strength $7.20 \times 10^5\ Pa$; the material properties for the femoral canal are : density $\rho = 1100\ kg/m^3$, Young's modulus $E = 2.28\ GPA$, Poisson's ratio $\nu = 0.3$ and yield strength $4.38 \times 10^4\ Pa$; while the
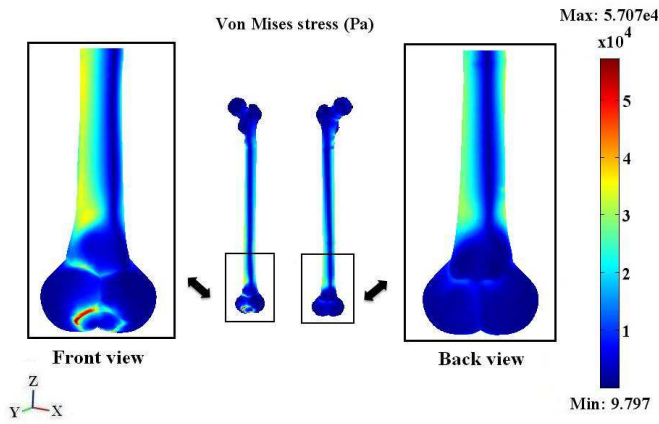
Fig. 10. Von Mises stress of the loading approximates the peak gait load for a 100 kg person during horizontal walking.

Fig. 11. Von Mises stress of the loading approximates the peak gait load for a 200 kg person during horizontal walking.
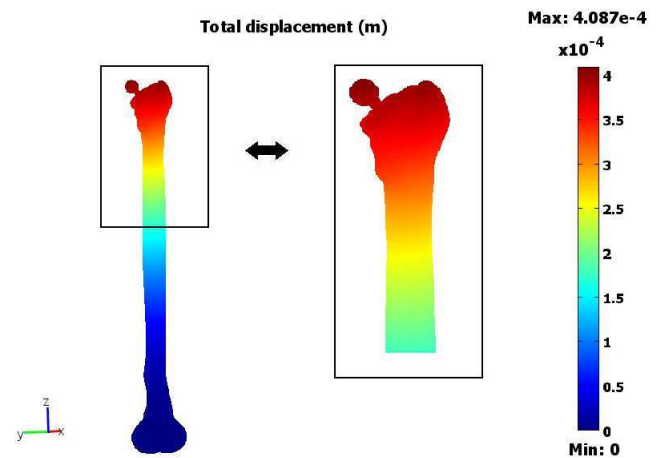
Fig. 12. Total displacement at a 70 kg person during normal walking.
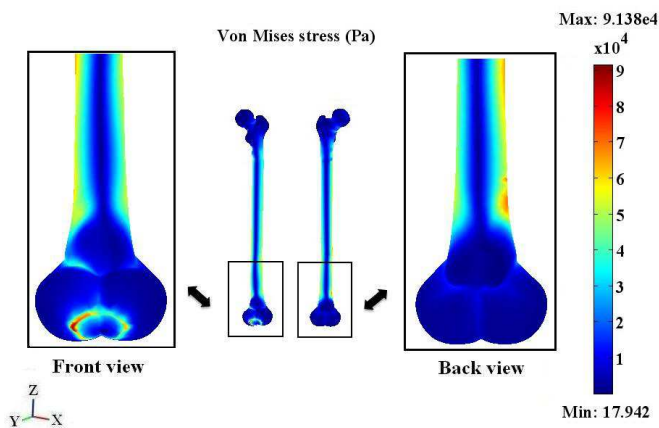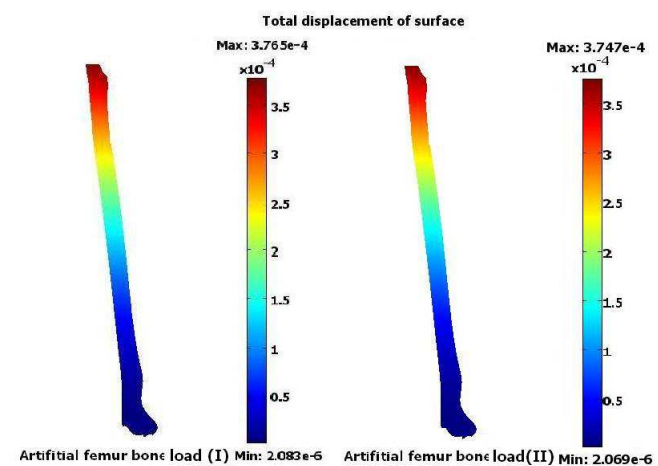
Fig. 13. Surface plot of the total displacement of artificial femur bone at load (I) and load (II).

material properties for the femur are : density ρ = 2000 kg/m^3, Young's modulus E = 2.13 GPA, Poisson's ratio ν = 0.3 and yield strength 1.48×10^8 Pa as shown in Table I– III.

In this part of study, we investigate the total displacement and von Mises stress for a 70 kg person during normal walk (I) and terminal stance horizontal walking (II). For the implant load (I) and implant load (II), the force acting on the object corresponding to patient's activity imposed at the head implant external point is simulated. On the distal epiphysis (the base) displacement is restrained.

For the implant load (I), we obtain that the total displacement of implant and femoral canal in artificial femur bone based on real domain for a 70 kg person during normal walk is $4.087e^{-4} \times 10^{-4}$ m.

Fig. 12 presents the total displacement of implant and femoral canal in artificial femur bone based on real domain for a 70 kg person during normal walking (I). The results show that high displacement appears at the head of implant and lower displacement occurs at the end of the femur. The surface plot of the total displacement for the different regions including artificial femur bone, femoral canal and

implant are compared in Fig. 13– 15. It is found that the total displacement of the implant is the largest. Fig. 16 shows the total displacement along the axial of artificial femur bone and femoral canal for a 70 kg person during normal walking. It indicates that the total displacement along the axial of artificial femur bone is larger than the along the axial of femoral canal. Von Mises stress as shown in Fig. 17– 19, indicates that high Von Mises Stress presents at the neck of the implant and femoral stem.

For the implant load (II), we obtain that the total displacement of implant and femoral canal in artificial femur bone based on real domain for a 70 kg person terminal stance during horizontal walking is $4.165e^{-4} \times 10^{-4}$ m. From the loading conditions, It can be seen the total displacement of second loading condition leads to much higher the total displacement of first loading condition.

V. CONCLUSION

The forces acting on the head and the end of the femur bone and implant in femoral canal have been studied numerically using a three-dimensional mathematical model and a numerical
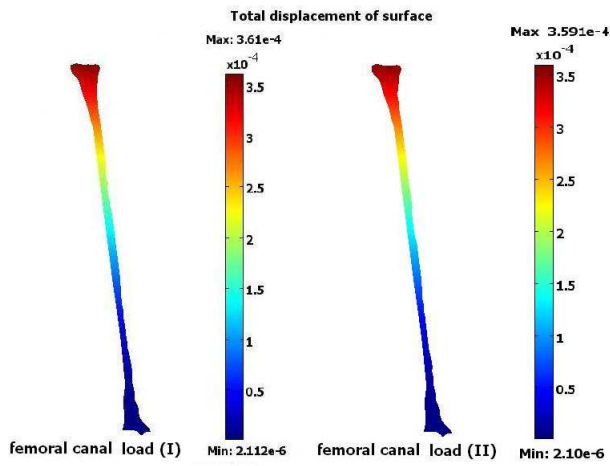
Fig. 14.   Surface plot of the total displacement of femural canal at load (I) and load (II).
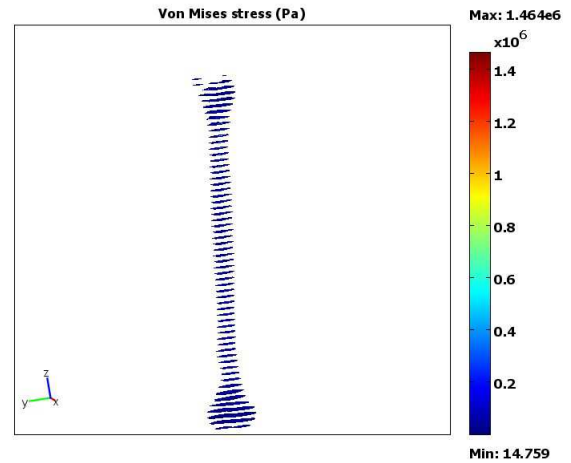
Fig. 17.   Von Mises stress for a 70 kg person during normal walking.
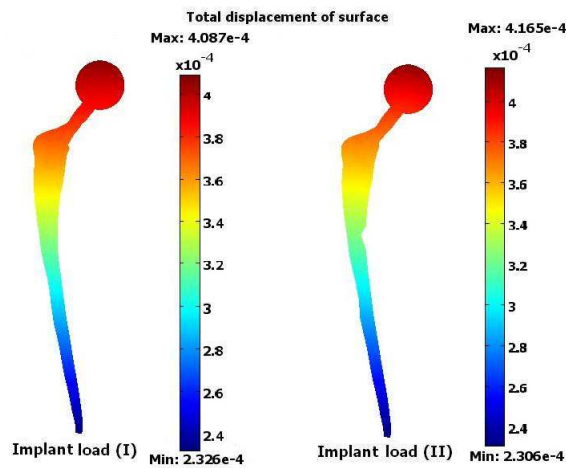
Fig. 15.   Surface plot of the total displacement of implant at load (I) and load (II).
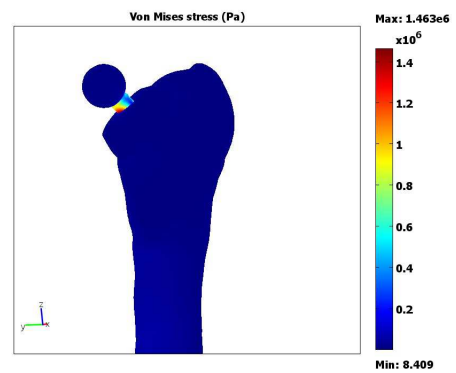
Fig. 18.   Von Mises stress for a 70 kg person during normal walking.
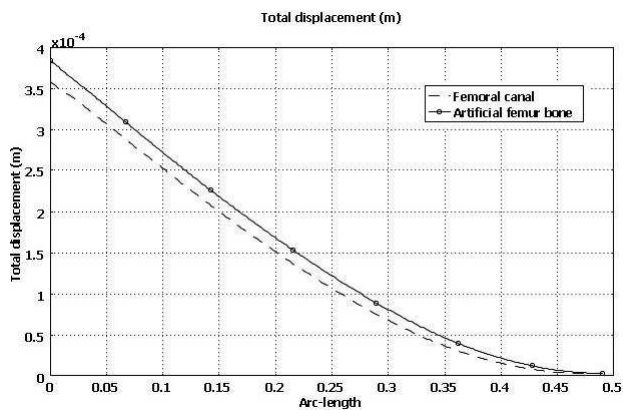
Fig. 16.   Profile of the total displacement along the axial of artificial femur bone where the solid-circled line, and the dashed line corresponds to the femoral canal for a 70 kg person during normal walking.
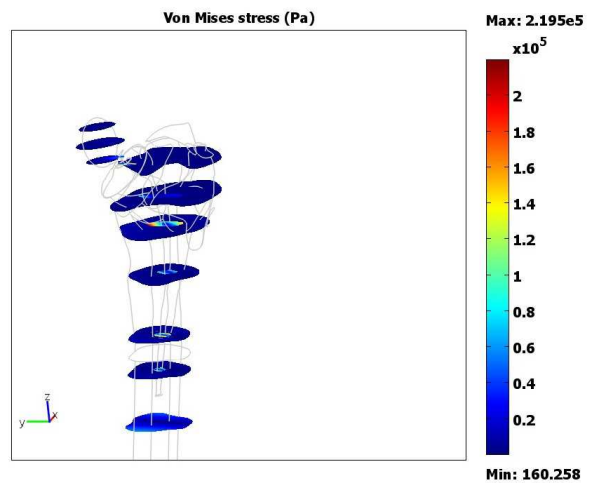
Fig. 19.   Von Mises stress for a 70 kg person during normal walking.

technique based on the finite element method. The numerical investigation shows that high displacement occurs at the head of the femur whereas the lower displacement occurs at the end of the femur. The results also show that higher weight provides higher total displacement. Moreover, it is found that the Von Mises stress affects the lateral femur. It should be noted that this paper focuses only on the static loads femur with implant. In the future, we will apply real geometry to simulate the cemented hip replacement with time dependent in order to obtain useful information and better understanding which could be of great help to orthopaedic surgeons.

REFERENCES

[1] J. Williams and N. Svensson, "An experimental stress analysis of the neck of the femur," *Medical and Biological Engineering and Computing*, vol. 9, pp. 479–493, 1971.

[2] S. Valliappan, N. Svensson, and R. Wood, "Three dimensional stress analysis of the human femur," *Computers in Biology and Medicine*, vol. 7, no. 4, pp. 253–264, 1977.

[3] A. Elkholy, D. Ghista, F. D'Souza, and M. Kutty, "Stress analysis of normal and osteoarthritic femur using finite element analysis," *International Journal of Computer Applications in Technology*, vol. 22, no. 4, pp. 205–211, 2005.

[4] T. Deshmukh, A. Kuthe, D. Ingole, and S. Thakre, "Prediction of femur bone geometry using anthropometric data of india population: A numerical approach," *International Journal of Medical Science*, vol. 10, no. 1, pp. 12–18, 2010.

[5] R. Fedida, Z. Yosibash, C. Milgrom, and L. Joskowicz, "Femur mechanical simulation using high-order fe analysis with continuous mechanical properties," in *II International Conference on Computational Bioengineering*, H. R. et al., Ed., Lisbon, Portugal, September 14-16 2005.

[6] A. Krauze, M. Kaczmarek, and J. Marciniak, "Numerical analysis of femur in living and dead phase," *Journal of Achievements in Materials and Manufacturing Engineering*, vol. 26, no. 2, February 2008.

[7] C. Precup, A. Naaji, C. Toth, and A. Toth, "Software simulation for femur fractures in case of frontal car accidents," *WSEAS Transactions on Computers*, vol. 7, no. 7, pp. 1050–1060, 2008.

[8] M. Pawlikowski, "Computer simulation of bone adaptation process under various load cases," in *Proceedings of the 2006 WSEAS international conference on Cellular and Molecular Biology, Biophysics and Bioengineering*. Athens, Greece: WSEAS, July 2006, pp. 117–122.

[9] N. G. Bizdoaca, D. Tarnita, D. Tarnita, D. Popa, and E. Bizdoaca, "Shape memory alloy based modular adaptive ortophedic impants," in *Proceedings of the 1st WSEAS International Conference on Biomedical Electronics and Biomedical Informatics*. Rhodes, Greece: WSEAS, August 2008, pp. 188–195.

[10] V. Volpe, C. Miraglia, L. Esposito, and M. Fraldi, "X-ray based technique for estimating bone fracture risk," in *Proceedings of the 2nd WSEAS International Conference on Biomedical Electronics and Biomedical Informatics*. Moscow, Russia: WSEAS, August 2009, pp. 244–246.

[11] S. Srimongkol and B. Wiwatanapataphee, "Simulations in cemented hip replacement," Ph.D. dissertation, Faculty of Science, Mahidol University, 2008.

[12] R. K. Hobbie and B. J. Roth, *Intermediate Physics for Medicine and Biology*, 4th ed. Springer, 2007.

[13] H. El-Sheikh, B. MacDonald, and M. Hashmi, "Material selection in the design of the femoral component of cemented total hip replacement," *J Mater Process Technol*, vol. 122, pp. 309–317, 2002.

[14] H. Katoozian and D. Davy, "Effects of loading conditions and objective function on the three-dimensional shape optimization of femoral components of hip endoprostheses," *Med Eng Phys*, vol. 22, pp. 243–251, 2000.